Medical Hypotheses 181 (2023) 111194

Contents lists available at ScienceDirect

Medical Hypotheses

journal homepage: www.elsevier.com/locate/mehy

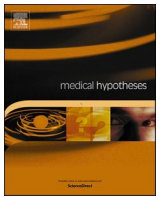

A mathematical model on Aβ blood–brain transport: Simulations of plaques' formation in Alzheimer's disease

Eleonora Ficiarà [a,*,1], Ilaria Stura [b,1], Caterina Guiot [b], Ezio Venturino [c,d]

[a] School of Pharmacy, Center for Neuroscience, University of Camerino, 62032 Camerino, MC, Italy
[b] Department of Neurosciences, University of Turin, Italy
[c] Department of Mathematics "Giuseppe Peano", University of Turin, Italy
[d] Member of the INdAM Research Group GNCS, Italy

ARTICLE INFO

Keywords:
Mathematical model
Numerical simulations
Alzheimer's disease
Amyloid Beta

ABSTRACT

In the process of toxic accumulation of Amyloid-beta (Aβ) peptides in plaques, problems may arise in the exchange of nutrients across the blood–brain barrier (BBB) level and impaired brain clearance. These plaques are associated with the progression of Alzheimer's disease (AD). A four-compartmental model to describe the alteration of Aβ transport across BBB level and its accumulation in the brain is presented here. Furthermore, potential target mechanisms of therapy, to counteract the disease progression, are investigated using an'in silico' approach. A sensitivity analysis is presented to show the most important parameters on which to act in order to potentially bring pathological conditions back to non-pathological ones.

Introduction

Background

Alzheimer's disease (AD) is a progressive and age-related neurodegenerative disorder, considered the major cause of dementia [1]. It is characterized by the loss of synapses and neurons and the two main hallmarks are the presence of extracellular plaques and intracellular neurofibrillary tangles, as underlined in a biomarkers' model [2]. Amyloid-beta (Aβ) peptide is the main protein composing the extracellular plaques, produced through the proteolytic processing of a transmembrane protein, amyloid precursor protein (APP), by β- and γ-secretases, and the main final Aβ forms are the 40-amino-acid ($A\beta$40) and the 42-amino-acid ($A\beta$42) [3]. The conversion of Aβ monomers into fibrillary aggregates is associated with the development of AD. Protein aggregation from soluble to insoluble structures has been considered a factor that may induce several neurological diseases and at times even to be toxic. Amyloid plaques predominating brain parenchyma mostly contain $A\beta$42, whereas cerebrovascular amyloid deposits primarily $A\beta$40 [4]. Furthermore, $A\beta$42 is considered more toxic than $A\beta$40 [5], and $A\beta$40 levels are not systematically assessed in many clinical laboratories alleging that this marker alone has no diagnostic value [6]. The cytotoxic effect of the $A\beta$42 peptide is believed to be linked to its ability to self-assemble to form oligomers and amyloid fibrils [7].

Two forms of AD have been characterized: familial and sporadic. The familial form is characterized by the alteration of specific genes. Missense mutations in presenilin 1 or 2 are the most common cause of early-onset AD, and presenilin is the catalytic subunit of γ-secretase. The mutations result in relative increases in the production of $A\beta$42/43 peptides. These hydrophobic species self-aggregate, leading to profound Aβ deposition in mid-life [8].

The main risk factor for sporadic AD is considered to be age, but other risk factors have been identified, such as the female sex, traumatic brain injury, depression, environmental pollution, physical inactivity, social isolation, low academic level, metabolic syndrome, and genetic susceptibility [9]. The ε4 allele of the apolipoprotein E (ApoE4) carriers was included in typical late-onset AD. This allele was found to markedly increase AD risk and decrease brain clearance of Aβ, leading to excess Aβ aggregation and typical downstream AD neuropathology [8].

Despite continuing debate about the Aβ hypothesis, new evidence worldwide supports the concept that an imbalance between the production and clearance of Aβ42 and related Aβ peptides is a very early, often triggering factor in AD.

Impaired brain clearance from the central nervous system (CNS) and

* Corresponding author.
E-mail addresses: eleonora.ficiara@unicam.it (E. Ficiarà), ilaria.stura@unito.it (I. Stura), caterina.guiot@unito.it (C. Guiot), ezio.venturino@unito.it (E. Venturino).
[1] These authors equally contributed to this work.

https://doi.org/10.1016/j.mehy.2023.111194
Received 11 July 2023; Received in revised form 7 October 2023; Accepted 20 October 2023
Available online 21 October 2023

the overproduction of Aβ in the brain are believed to be responsible for plaque formation [10]. On the other hand, cerebrospinal fluid (CSF) levels of $A\beta42$ are used for the diagnosis of AD. It is important to note that AD patients present decreased values of $A\beta42$ in the CSF concerning non-AD, and consequently, low $A\beta42$ is considered to be a positive biomarker for AD [11]. Aggregation of $A\beta42$ appears the most likely cause for the decreased $A\beta42$ concentration in CSF in AD: the aggregated state inhibits $A\beta42$ from being transported from the interstitial fluid (ISF) of the brain to the CSF [11]. Moreover, the presence of Aβ plaques is associated with a decrease in the ISF and CSF concentrations of $A\beta42$, a decrease in the blood–brain barrier (BBB)/proteolysis fluxes of $A\beta42$, and an increase in deposition flux of $A\beta42$ [12]. Plaques formation can be caused by deficient transport efflux mechanisms at the BBB level: a faulty brain degradation or an increased influx of circulating Aβ across the BBB. The BBB is a dynamic physiological interface between the plasma and the brain, mediating Aβ transport between these two compartments. The BBB is crucial in maintaining the normal metabolism of Aβ, and its dysfunction aggravates Aβ deposition [13,14]. Specialized receptors at the BBB shuttle Aβ across the brain endothelium from the CNS into the bloodstream or from the blood into the CNS. The receptor for advanced end glycation products (RAGE) and low-density lipoprotein receptor-related protein 1 (LRP) remain the primary targets, as shown by their ability to rapidly transport free circulating Aβ into the CNS and brain-derived Aβ into the blood [15,16].

Due to the involvement of Aβ in the pathogenesis of AD, there is a growing interest in the investigation of the temporal dynamics of Aβ and the factors associated with its conversion/aggregation mechanisms in the brain [17].

Mathematical models of the Aβ kinetics provide a good mechanistic understanding of the Aβ accumulation in the brain, helping to predict potential effects on health. Several mathematical models investigate Aβ trafficking and accumulation at the BBB endothelium [18], the aggregation of Aβ monomers into oligomers [19], and also how sleep may affect Aβ fibrillation [20]. However, these mathematical models usually refer to a very short time scale (one day) to describe each exchange between compartments accurately. Indeed, they cannot be used to study phenomena that require long periods of formation (years), such as accumulation of Aβ plaques, and corresponding long observation times.

The hypothesis

In view of the above-mentioned studies proving that Aβ is a dominant factor of AD pathogenesis, the hypothesis proposed in this work is that the involvement of Aβ in AD is due to the interplay between impaired Aβ transport across brain barriers and the process of plaques aggregation in the brain.

This fits with the literature evidence in which many different mechanisms have been postulated as significant factors in AD pathogenesis, especially plaques accumulation and impaired Aβ brain clearance. A better understanding of the temporal dynamics of these processes (by in silico approaches) is critical for guiding experiments aimed at the development of more effective therapeutic agents that target the underlying disease mechanisms.

Hence, this work aims to build a mathematical model of the Aβ transport across BBB and the plaques formation process in the brain. To do this, a compartmental model is created, composed of four compartments describing the exchange between blood and brain environment, setting the parameters based on biological mechanisms from literature and on our previous data [21,22]. Finally, numerical simulations are performed to reproduce physiological and pathological conditions, to assess what processes mainly affect Aβ concentrations for the AD condition, and to identify potential target mechanisms of therapy.

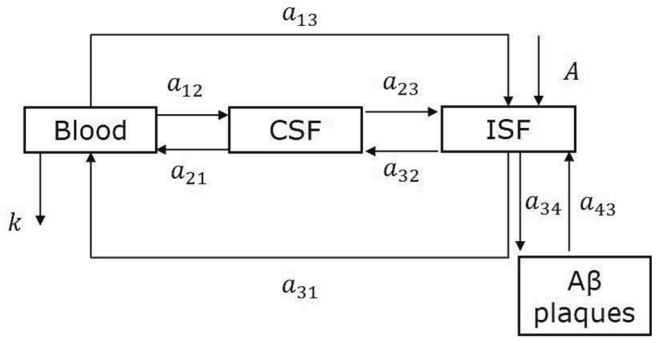

Fig. 1. Schematic representation of the four compartmental models describing the passage of Aβ between blood and brain and the potential toxic accumulation of Aβ plaques in the brain environment.

Materials and methods

Model description

The present model is an extension of our previous models on iron transport across the BBB [21,22], adding a specific compartment for the formation of Aβ plaques. Therefore, four compartments are modeled: blood B, the cerebrospinal fluid CSF, the interstitial fluid ISF, and the Aβ plaques P.

$$\frac{dB}{dt} = -(a_{12}+k+a_{13})B(t)+a_{21}CSF(t)+a_{31}ISF(t) \tag{1}$$

$$\frac{dCSF}{dt} = a_{12}B(t)-(a_{21}+a_{23})CSF(t)+a_{32}ISF(t) \tag{2}$$

$$\frac{dISF}{dt} = a_{13}B(t)+a_{23}CSF(t)-(a_{32}+a_{31})ISF(t)-a_{34}CSF(t)P(t)^{\frac{2}{3}}+a_{43}P(t)+A \tag{3}$$

$$\frac{dP}{dt} = a_{34}ISF(t)P(t)^{\frac{2}{3}}-a_{43}P(t) \tag{4}$$

The first equation $B(t)$ represents the Aβ in the systemic blood; the second and the third equations represent the Aβ concentrations in CSF and ISF respectively, i.e., two fluids present in the brain; the last one represents the Aβ plaques in ISF, where Aβ is heavily deposited in pathological cases (see Fig. 1).

Note that there are links among all these compartments, so that the Aβ peptides may migrate from one to the other. The compartment of the plaques P is part of the ISF in the brain and it communicates directly only with the ISF. Because the plaques are three-dimensional conglomerates, they can increase in size as new particles are added, coming into contact with them. To model this hypothesized feature, the growth of the conglomerate must be proportional to its surface. Because the plaque is a three-dimensional object, an exponent of 2/3 is used to account for the growth rate as explained below.

The use of a fractional exponent represents indeed the main novelty of our model. As mentioned, it indicates the interaction of soluble Aβ in ISF with the surface of the associated plaques in the space of three dimensions. The soluble Aβ attaching to the surface of the plaques makes them grow in size. The arrows in the diagram are directed, indicating the allowed direction of the flow (see Fig. 1).

All the coefficients are assumed to be positive and constant. The parameters A, a_{34}, a_{43}, a_{21}, a_{32}, a_{13}, a_{31}, and k are assumed to be different between the two conditions of AD and non-AD patients. The coefficients $a_{i,i\pm1}$, $i = 1, 2, 3$ describe the flow of Aβ between compartments i and $i \pm 1$, namely B, CSF, and ISF, while a_{34} and a_{43} denote the in and outflow between ISF and the plaques. Indeed, the Aβ peptides are endogenously produced by the brain and a continuous inflow into ISF at rate A is assumed. In particular, a_{34} indicates the formation of the

Table 1
Table of parameters used for the simulations.

Neurological control condition		AD condition	
Parameters	Initial conditions	Parameters	Initial conditions
$a_{12} = 0.01$	$B = 15.5$	$a_{12} = 0.01$	$B = 13.3$
$a_{21} = 0.05$	$CSF = 600$	$a_{21} = 0.03$	$CSF = 600$
$a_{23} = 0.02$	$ISF = 600$	$a_{23} = 0.02$	$ISF = 600$
$a_{32} = 0.08$	$P = 0$	$a_{32} = 0.05$	$P = 0$
$a_{34} = 0.00005$		$a_{34} = 0.005$	
$a_{43} = 0.0001$		$a_{43} = 0.0001$	
$a_{13} = 0.3$		$a_{13} = 0.5$	
$a_{31} = 0.01$		$a_{31} = 0.005$	
$k = 2$		$k = 0.4$	
$A = 69.0$		$A = 90.0$	

plaques, while a_{43} the dissolution of the Aβ plaques and their return to the soluble state in the brain. In AD patients, a_{34} is larger than in non-AD ones, while a_{43} is very small in all the patients because there is a low probability of plaque dissolution. The constant k describes *clearance*, which consists of the protein destruction by excretory mechanisms in the systemic blood.

The parameters a_{21} and a_{32} can be related to the turnover and clearance of Aβ within the brain, especially the complex flow and exchange of *CSF* and *ISF*, known as "glymphatic" fluxes, (i.e., flow within the perivascular space and brain interstitium resulting in mixing of *CSF* and *ISF*) [12]. These parameters are lower in AD conditions due to the decline of Aβ clearance from the brain.

The parameters a_{13} and a_{31} reflect the exchange mechanisms between the blood and brain compartments. They could be related to the receptors on the BBB, such as the activity of LRP and RAGE, which could be altered in the AD process [16]. The parameters for numerical simulations were set based on biological processes and values reported in the literature [15,18,23–25] and our previous data in *Aβ42 CSF* of patients affected by dementia and neurological controls [26].

All the simulations were performed using our own developed codes in Matlab © 1994–2022 The MathWorks, Inc.

Equilibria

The system stationary points are found by the equilibrium equations. The only two possible cases are analyzed below. As far as the equilibrium in the absence of plaques is concerned, the point is

$$\widehat{E} = \left(\frac{A}{k}, \frac{A}{k}\frac{a_{12}(a_{32}+a_{31}) + a_{32}(k+a_{13})}{a_{21}a_{32}+a_{31}a_{21}+a_{31}a_{23}}, \frac{a_{13}A + (kA + a_{23}\widehat{x}_2)}{a_{32}+a_{31}}, 0\right),$$

while in the presence of plaques, it becomes

$$E^* = \left(\frac{A}{k}, \frac{A}{k}\frac{(ka_{32}+a_{12}a_{32}+a_{12}a_{31}+a_{32}a_{13})}{(a_{21}a_{32}+a_{31}a_{21}+a_{31}a_{23})}, \frac{A}{k}\frac{(ka_{21}+ka_{23+}a_{12}a_{23}+a_{21}a_{13}+a_{23}a_{13})}{(a_{21}a_{32}+a_{31}a_{21}+a_{31}a_{23})}, \left(\frac{A}{k}\frac{a_{34}(ka_{21}+ka_{23+}a_{12}a_{23}+a_{21}a_{13}+a_{23}a_{13})}{a_{43}(a_{21}a_{32}+a_{31}a_{21}+a_{31}a_{23})}\right)^3\right)$$

Because all the parameters are positive, the above components of the two equilibria are non-negative, thereby ensuring their unconditional feasibility. Further details on the equilibria derivation can be found in Appendix A. The other possible system equilibria are unconditionally infeasible. These points are therefore excluded from further analysis. Further details on the equilibria local stability analysis can be found in Appendix B. As a general result, the plaque-free point cannot be attained, because it is unconditionally unstable. When locally asymptotically stable, it follows that the coexistence equilibrium is also globally asymptotically stable.

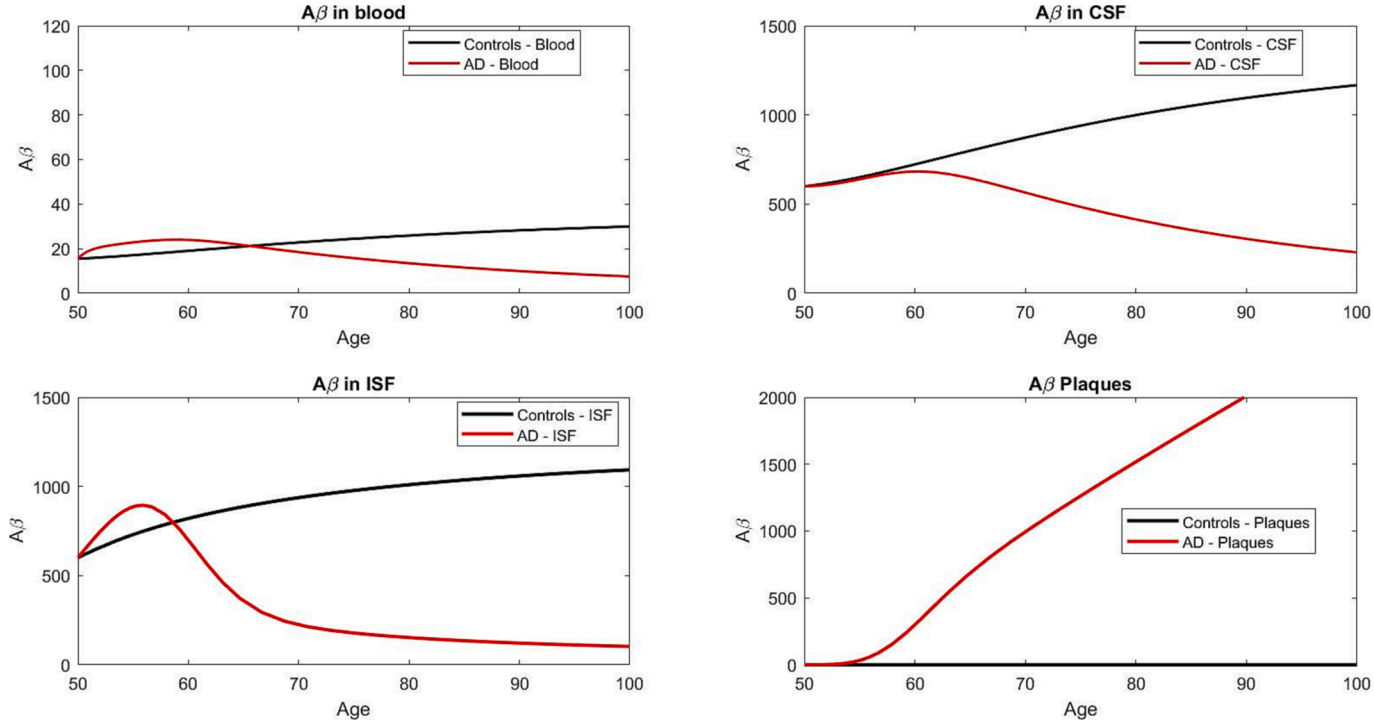

Fig. 2. Simulations for the four compartments using parameters shown in Table 1 for neurological control (black line) and AD (red line) conditions.

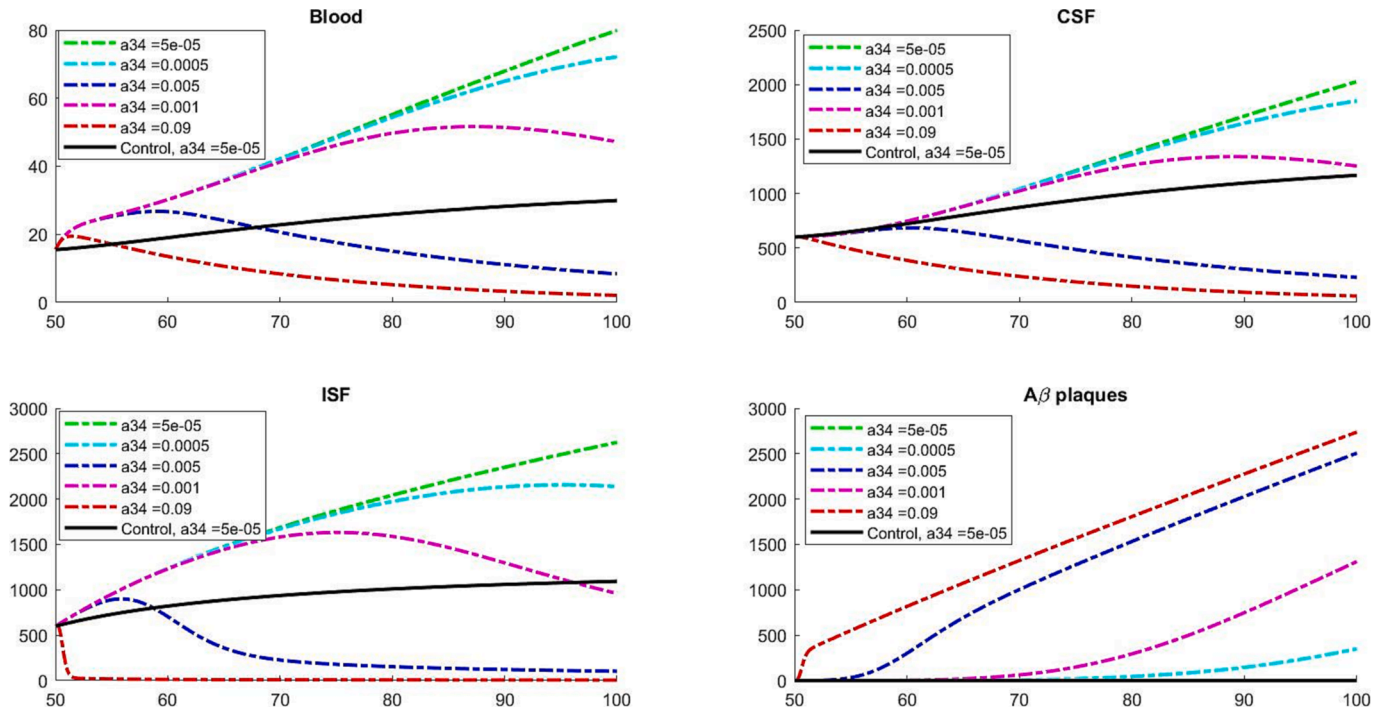

Fig. 3. Simulations changing the parameter a_{34} in the range $0.00005 < a_{34} < 0.09$ for AD condition. Simulation for control condition in each compartment is shown (black line).

Sensitivity analysis

Sensitivity analysis aims to focus on the parameters that, alone or in combination with other ones, can dramatically change the equilibrium of the model. In other words, the range of the parameters that possibly lead to a regression of the pathological situation to a normal one is investigated. The basic idea is to understand which biological mechanism should be corrected with a hypothetical drug to invert a pathological situation.

To understand the weight of each single parameter in the model, many simulations were performed, varying the value of one or two parameters simultaneously.

Sensitivity analysis was performed as follows: for each parameter, a possible range of values was considered, referring to literature. Fixing all the other parameters at the level prescribed by the AD condition (see Table 1), a simulation was performed with different values of the first parameter, ranging in the chosen interval. Moreover, simultaneous variations of the combination of two parameters were considered, to evaluate potential correlated effects. All the parameters of the model were analyzed. Only the most significant impacts are depicted in the

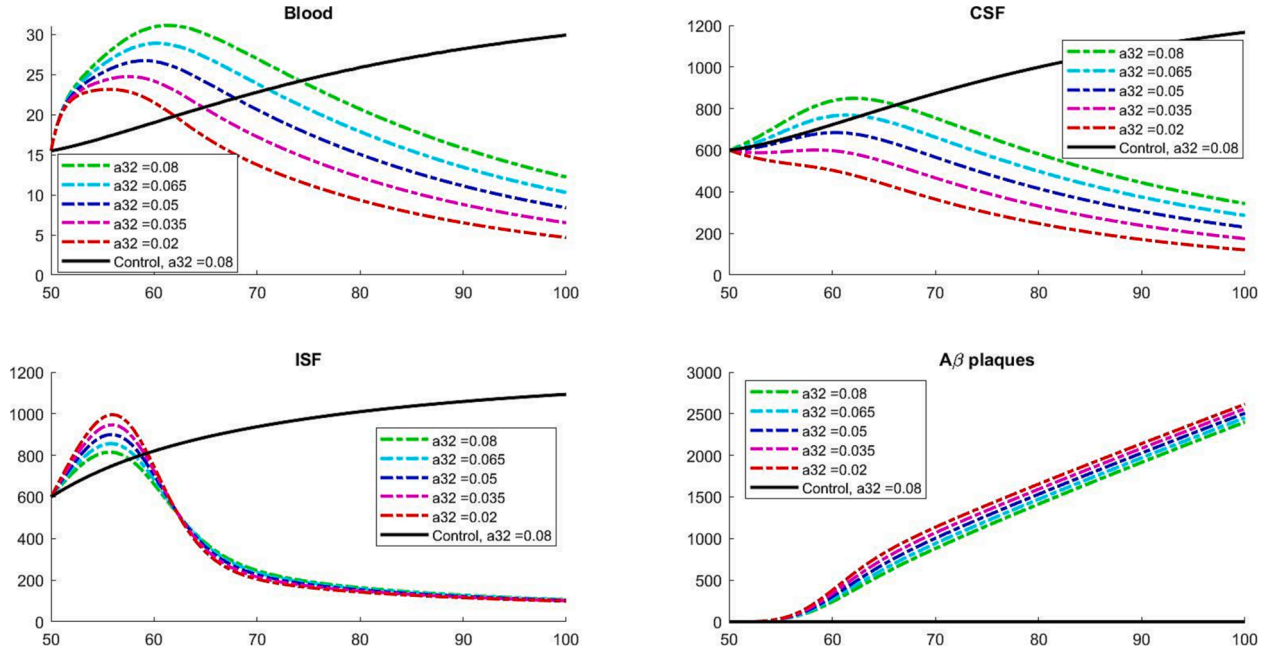

Fig. 4. Simulations changing the parameter a_{32} in the range $0.02 < a_{32} < 0.08$ for AD condition. Simulation for control condition in each compartment is shown (black line).

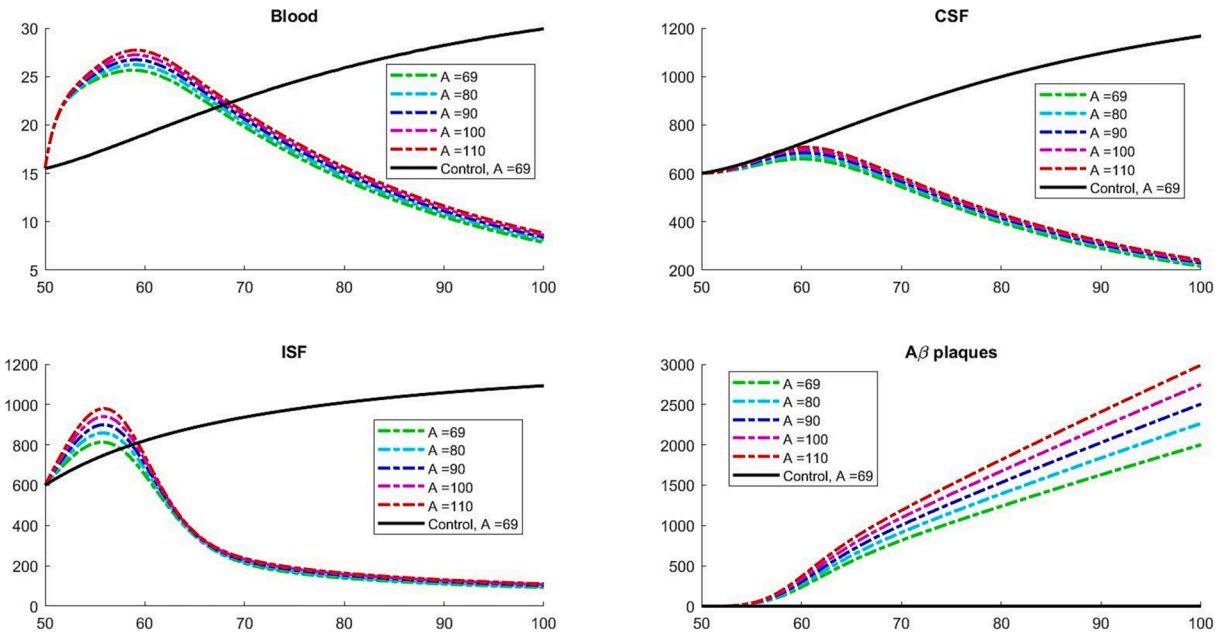

Fig. 5. Simulations changing the parameter A in the range $69 < A < 110$ for AD condition. Simulation for control condition in each compartment is shown (black line).

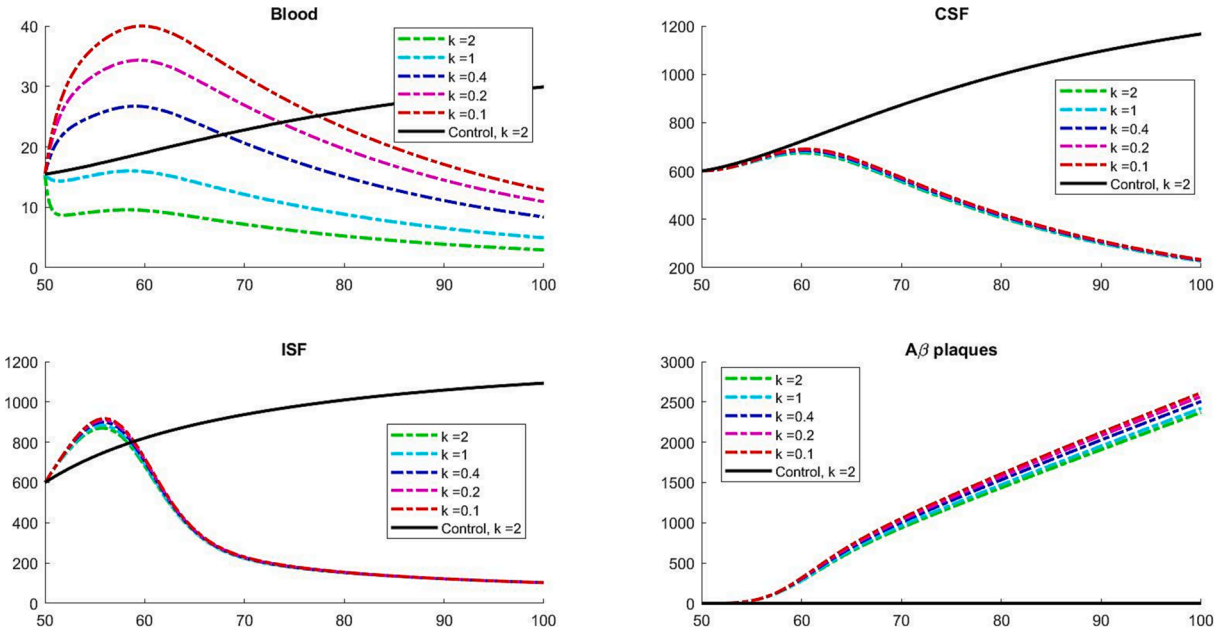

Fig. 6. Simulations changing the parameter k in the range $0.1 < k < 2$ for AD condition. Simulation for control condition in each compartment is shown (black line).

Results section.

Results

Simulations of pathological and control conditions

The values used for the parameters are listed in Table 1. Due to the strict contact between *CSF* and *ISF*, the same initial conditions are set in the two compartments (see Table 1). Initial values of Aβ in the blood are obtained from literature [23].

Fig. 2 shows the results of the simulations. The various frames contain the Aβ concentrations in the four compartments in the case of AD (red lines) and non-AD (black lines) conditions. On the horizontal axis, the patient age is shown (in the range of 50–100 years), while the vertical one contains the Aβ concentrations in the liquids for the first three compartments and the amount of Aβ plaques (in pg/ml) in the last frame.

As hypothesized, Aβ concentration decreases in the blood compartment in the AD condition, while it has a slight increase in the control one. The same trend is shown also in the *CSF* and *ISF* compartments, while in the fourth one, an opposite behavior is present. Indeed, Aβ is transformed into plaques in the AD condition, while no conglomerates are created in the control one.

The values of equilibrium points are not attained during the simulation time ($E_{Control} = (34.5, 1357.2, 1183.3, 2.0 \bullet 10^8)$, non-AD patients; $E_{AD} = (225, 5856.4, 5811.4, 2.4 \bullet 10^{16})$, for AD).

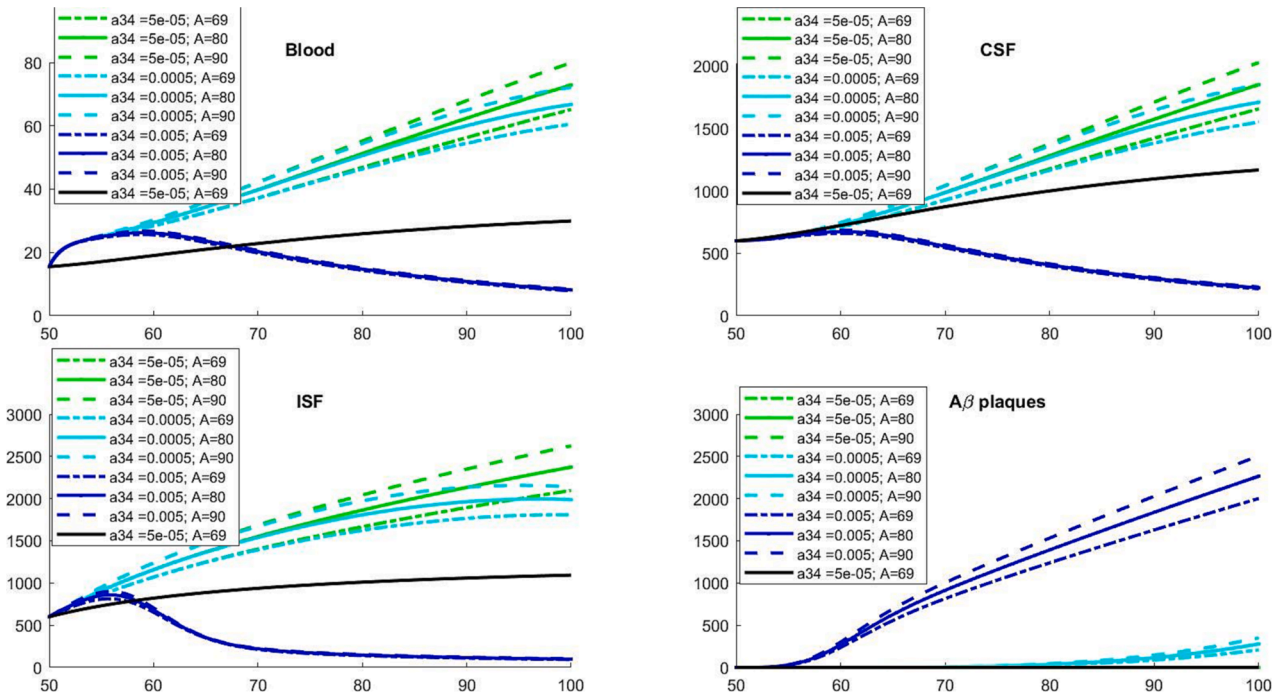

Fig. 7. Simulations changing the parameters a_{34} and A. Simulation for control condition in each compartment is shown (black line).

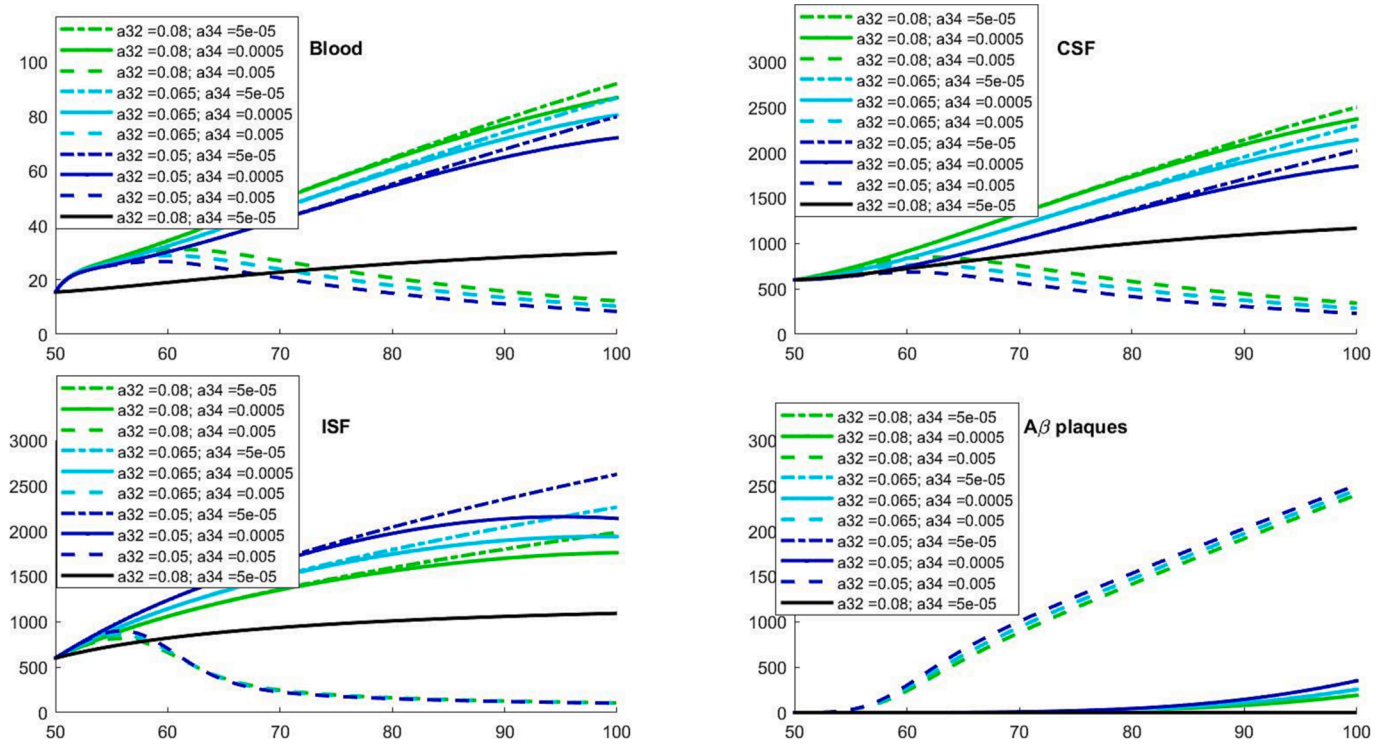

Fig. 8. Simulations changing the parameters a_{32} and a_{34}. Simulation for control condition in each compartment is shown (black line).

In-silico investigation of possible therapies

In this section, we perform simulations assuming that drugs can be developed to potentially impair the fluxes between compartments. In such situations, it would be important to know how changing such fluxes could affect the system behavior, with the ultimate goal of restoring the AD condition to the normal neurological situation, if at all possible. Therefore, the numerical experiments aim to assess how each flux, starting from the pathological conditions, modifies them in a favorable direction. We concentrate on two cases, the influence of each single flux as well as suitably chosen pairs of parameters. To evaluate which parameters mainly affect $A\beta$ concentrations for the AD condition, at first simulations varying one parameter at a time are performed. The parameters range used is based on Table 1 for both neurological control and AD conditions. In all the figures, the initial value for the parameter is chosen to roughly agree with the pathological conditions, as explained

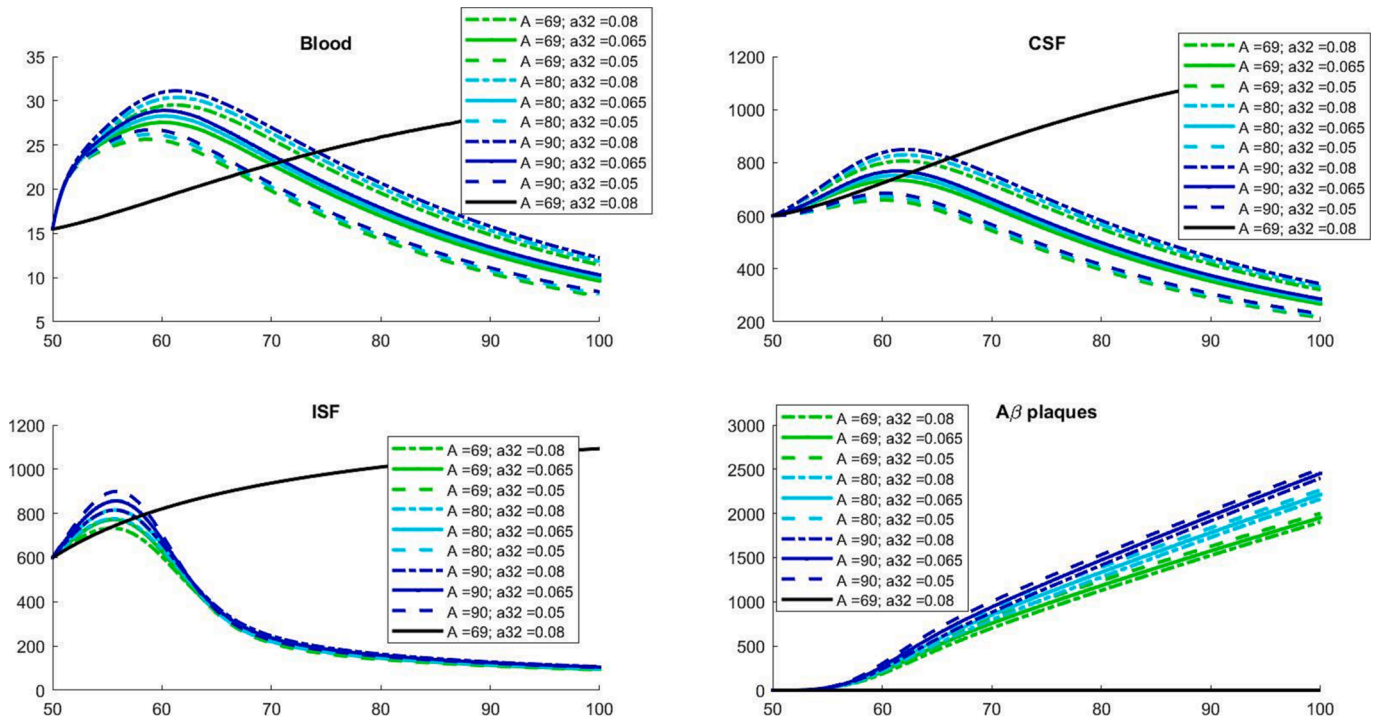

Fig. 9. Simulations changing the parameters a_{32} and A. Simulation for control condition in each compartment is shown (black line).

in Section Sensitivity Analysis.

Figs. 3–6 show the concentration of $A\beta$ in the four compartments for different values of a_{34}, a_{32}, A, and k respectively. Figures related to parameters a_{13}, a_{31}, and a_{21} are shown in Appendix C.

The parameter a_{34} heavily affects the $A\beta$ concentration in all compartments (Fig. 3). Changing the value of this parameter, the pathological condition could be modulated. In particular, lowering its value, the concentration of $A\beta$ plaques approaches the curve of the control condition (Fig. 3). Just varying the parameter a_{32} instead does not give a good result; the $A\beta$ concentration in *CSF* can be modulated (Fig. 4), but ultimately they remain far from the non-pathological conditions.

A similar result is obtained by acting on the parameter A alone. This parameter affects the formation of $A\beta$ plaques in a pathological condition, especially in the initial part of the progression of the disease (Fig. 5), in which the formation of plaques could be modified to approach the non-AD condition.

The parameter k seems to impact mainly on the $A\beta$ concentration of the blood (Fig. 6). Based on the simulations, it appears that a therapy acting on the parameter a_{34}, and in a minor way on a_{32} and A, may have a role to counteract the formation of $A\beta$ plaques.

Simultaneous variations of a combination of these parameters are then considered, to evaluate potential correlated effects.

Fig. 7 shows the strong influence of the higher values of the parameter a_{34} concerning those of A. The latter negatively affects the concentration of $A\beta$ in a significant way when a_{34} has lesser values. These results support those obtained in Fig. 3 and show that high values of a_{34} are not significantly altered by high values of A. Fig. 8 combines the changes of a_{34} and a_{32}. The undesired behavior occurs in three specific cases, in which a_{34} has the highest value 0.005, independently of the values attained by a_{32}. Therefore, the bad behavior inherited by $a_{34} = 0.005$ alone in Fig. 3 cannot be altered by operating on the parameter a_{32}. Conversely, using a_{34} as a control, the bad behavior observed for all the values in the range for a_{32} in Fig. 4 can be corrected using low values of a_{34}.

Finally, the pair a_{32} and A is shown in Fig. 9. The simultaneous variations of a_{32} and A, do not significantly change the bad behavior due to the parameter a_{32} observed in Fig. 4. The concentration of a_{32} affects the compartments of blood *B*, *CSF,* and *ISF*, while parameter A seems to impact the $A\beta$ plaques concentration, with low values attaining smaller concentrations. However, the latter remains far too high, especially for the most aged individuals.

Discussion

In this work, a model to potentially describe the Aβ transport across the BBB level and the accumulation of Aβ plaques in the brain environment in AD and non-AD conditions is proposed and analyzed.

In the first simulations, Aβ concentration in blood (Fig. 2, top left) has very few variations in both cases (AD and neurological control condition), remaining in a range of 10–40 pg/ml. This can be comparable to values reported in the literature for plasma levels of Aβ [27]. An increment of Aβ values in *CSF* (top right) and *ISF* (bottom left) for non-AD patients and a decrement for AD ones are shown, coherently with literature data [11,23,26]. It is widely accepted that the negative correlation between amyloid plaque density and CSF-Aβ42 occurs because senile plaques create a sink for extracellular soluble Aβ42 [28] and the difference in CSF-Aβ42 between AD patients and subjects with normal cognition is in the range of 500 pg/ml [29]. The threshold of 500 pg/ml is considered as the limit for the classification of AD patients in several methods of clinical analysis. The results reveal that this condition in *CSF* is reached in the age range of 60–70, i.e., when the AD condition is more frequently diagnosed.

Aβ plaques concentration grows rapidly in AD simulations, while they do not develop in neurological controls.

As far as the equilibrium points are concerned, they are not attained during the simulation time. The time it takes to reach these equilibrium values is far greater than human life. This is plausible from a physiological point of view. Indeed, this delicate mechanism we have tried to describe is based on small dynamical adjustments over the years and does not attain equilibrium. In fact, it is established that Aβ deposition is slow and protracted, likely to extend for more than two decades, with a time frame of Aβ accumulation of 19.2 years from threshold to onset of dementia [30].

Several works compared the total amount of Aβ in AD and control

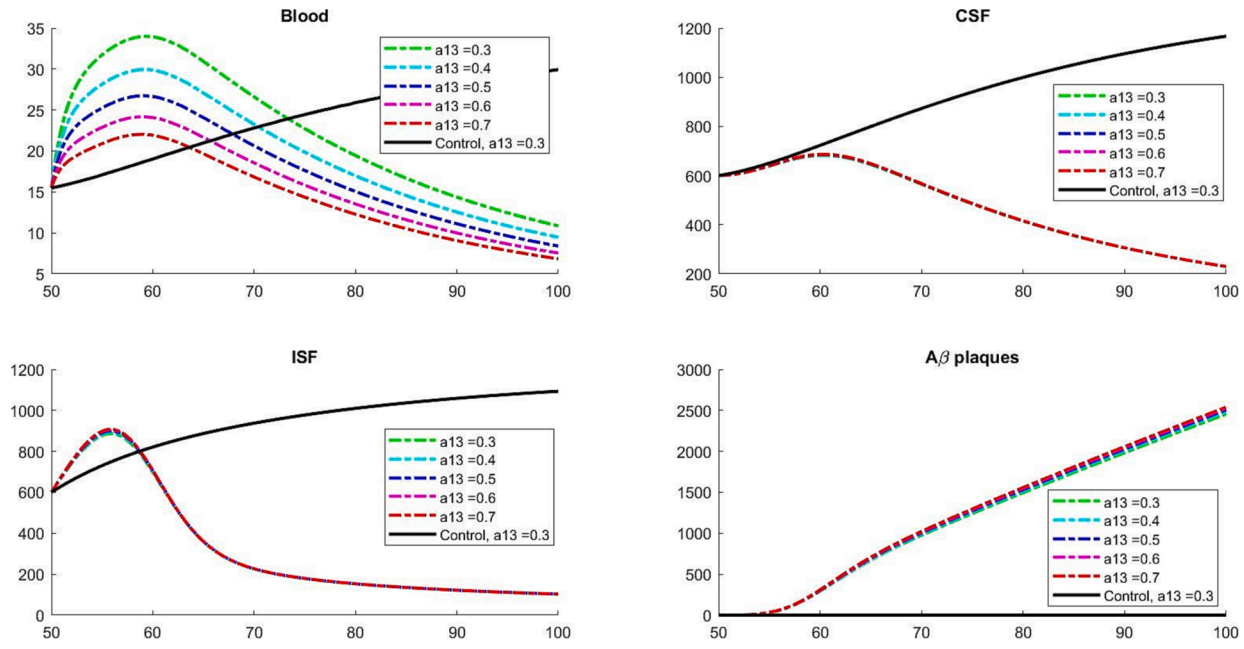

Fig. 1a. Simulations changing the parameter a_{13} in the range $0.3 < a_{13} < 0.7$ for AD condition. Simulation for control condition in each compartment is shown (black line).

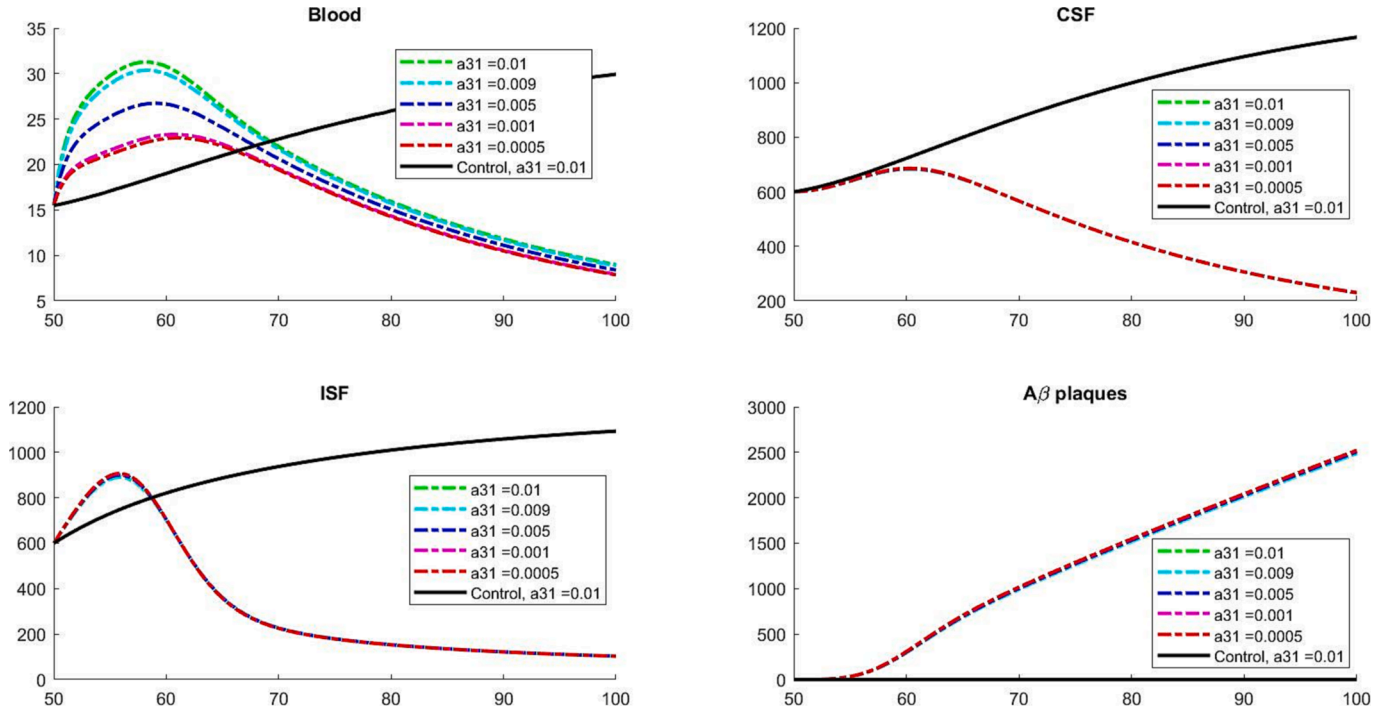

Fig. 2a. Simulations changing the parameter a_{31} in the range $0.0005 < a_{31} < 0.01$ for AD condition. Simulation for control condition in each compartment is shown (black line).

brains. Roberts and colleagues showed that in AD brain there was an average total of 6.5 ± 5.0 mg Aβ compared to control brain 1.7 ± 2.3 mg, estimating also the rates of accumulation of Aβ in a subject set to develop AD [31]. Hampel et al. thoroughly reviewed Aβ biochemical properties from monomers through higher aggregation states, including plaques, typically viewed as an AD neuropathological hallmark [32].

Therefore, the model introduced here conforms to known physiological evidence and could be useful in understanding the mechanisms behind the formation of the Aβ plaques. In addition, our in-silico simulations (see section In-silico investigation of possible therapies) may indicate the possible targets of new therapies, aimed at suitably modifying the compartmental flow rates to reduce or hopefully stop the progression of the disease.

Sensitivity analysis suggests that the parameter a_{34} (reflecting the process of plaques formation) strongly affects the formation of Aβ plaques (Fig. 3). Modulating this parameter could impact the progression of the disease. Also, the parameter a_{32} (corresponding to the efflux of Aβ from the brain to the CSF) seems to modulate the Aβ concentration in CSF, supporting the hypothesis of reduced clearance from the brain in AD condition, but this occurs to a much lesser extent. In particular, this

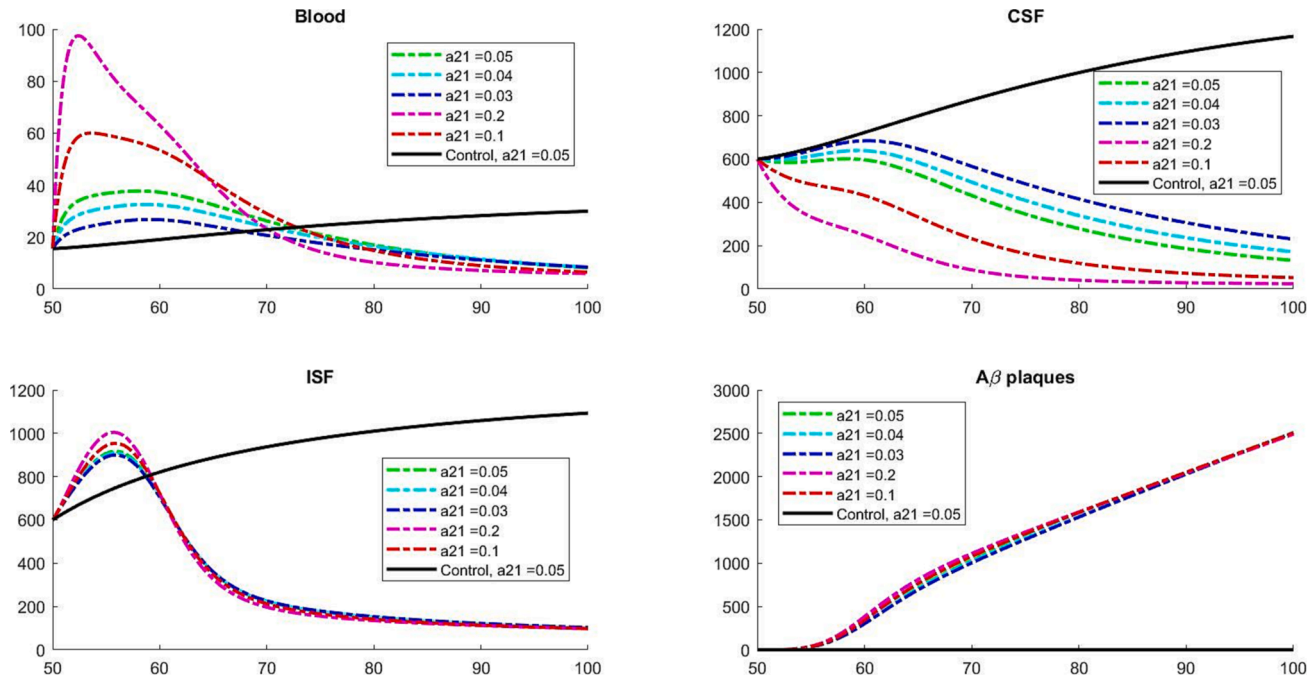

Fig. 3a. Simulations changing the parameter a_{21} in the range $0.05 < a_{21} < 0.1$ for AD condition. Simulation for control condition in each compartment is shown (black line).

parameter can be related to CSF-based Aβ clearance, which could change during the aging process [12,33].

Our model results suggest that it should be crucial to investigate the role of transporters involved in the Aβ transport at the brain's barriers and relative alteration, i.e., using in vitro experiments, to develop effective transporter-targeting for therapy. For example, the family of ABC transporters is considered for potential treatment of AD [34].

Furthermore, the parameter k tunes the Aβ blood levels, as underlined by sensitivity analysis. It seems not to be relevant for the formation of the plaques. However, recent evidence highlights that understanding the clearance mechanism of Aβ in the periphery of blood circulation turns out to be important for the development of effective therapies for AD [35]. Probably, a relevant effect for changes of this parameter in the brain environment needs to be supported by variations of other parameters. In addition, the simulations obtained varying two parameters simultaneously suggest potential correlations between parameters and their effect, especially for a_{34} and A. In fact, in our model, these latter indicate two important processes for the accumulation of the plaques: the formation (reflected in a_{34}) and the production of Aβ in the brain environment (indicated from A). Tuning these two parameters could have an impact on the formation of the plaques, suggesting potential targets for therapy acting on these processes to counteract AD progression. It could be of interest for the prediction of the disease to estimate these parameters from the clinical analysis point of view.

Mathematical models in the literature focus on different processes affecting the accumulation of Aβ in the brain. Wang and colleagues investigated the accumulation kinetics of Aβ in the BBB endothelium, such as brain-to-plasma efflux kinetics, highlighting the importance of BBB trafficking in regulating plasma and $A\beta 42/40$ ratios, disrupted in dementia [18]. Furthermore, a discrete-time mathematical model for the aggregation of Aβ monomers into oligomers using concepts from chemical kinetics and population dynamics is proposed [19], presenting a formula for the reduction of the aggregation of monomers to the toxic oligomers. This is in agreement with our results about the strong impact of the variations of a_{34} (the parameter related to Aβ aggregation) in the process of plaque formation and consequently on the disease progression.

A limitation of this work is the impossibility of validating the model with real longitudinal clinical data, even if literature information is used and compared with simulations. Moreover, there is not yet clinical evidence for the estimation of parameters, which makes it difficult to use the model in the context of personalized medicine. However, this type of validation and usage is beyond the scope of this paper.

Methods to assess the viability of our suggested hypothesis could be performed both in vitro and *in vivo*. For example, testing how alterations of transporters located at brain-barrier levels can affect the formation of the plaques in *in vitro* models. On the other hand, *in vivo* models (i.e., animal models) could better capture the complexity of the mechanisms measuring the Aβ concentrations in blood and CSF during the progression of the disease, allowing also parameter estimates of the model. This measure could validate the temporal dynamics of our models.

Conclusions

In this paper, a macroscopic model is presented, hypothesizing the behavior of Aβ in the brain, gathering potential BBB dysfunctions and a possible explanation of the plaques formation mechanism in non-AD and AD conditions.

Using an in silico approach, it also proposes an analysis of the major impacting parameters, which could be translated into biological knowledge. The model especially reveals the importance of Aβ aggregation into plaques in the brain and the impaired clearance mechanism from the brain, two of the factors causing the toxicity leading to neurodegeneration.

This analysis could ultimately serve as a roadmap to formulate new experiments on potential therapies against AD progression.

Funding statement

Ex-post grant 2020 (GUIC_S1921_EX-POST_21_01) from the University of Torino and Compagnia di San Paolo.

Declaration of Competing Interest

The authors declare that they have no known competing financial interests or personal relationships that could have appeared to influence

the work reported in this paper.

Appendix A. The coexistence equilibrium

For the coexistence point $E^* = (x_1^*, x^*_2, x^*_3, x^*_4)$ summing the third and the fourth equilibrium equations, we obtain

$$a_{13}x_1 + a_3x_2 - (a_{32} + a_{31})\,x_3 + A = 0$$

To this equation we add the first equilibrium equation and subtract the second one, obtaining, after simplification:

$$x_1^* = \frac{A}{k}$$

the same value obtained for equilibrium *E*. Substituting this value into the first two equilibrium equations, and solving them for x^*_3 we find

$$x_3 = \left[\frac{A}{K}(a_{12} + k + a_{13}) - a_{21}x_2\right]\frac{1}{a_{31}} = \frac{(a_{21} + a_{23})x_2}{a_{32}} - \frac{a_{12}A}{a_{32}k}$$

which allows determining the value of x^*_2,

$$x_2^* = \frac{A(ka_{32} + a_{12}a_{32} + a_{12}a_{31} + a_{32}a_{13})}{k(a_{21}a_{32} + a_{21}a_{31} + a_{23}a_{31})}$$

and back substitution gives immediately the value of x^*_3

$$x_3^* = \frac{A(ka_{21} + ka_{23} + a_{12}a_{23} + a_{21}a_{13} + a_{23}a_{13})}{k(a_{21}a_{32} + a_{21}a_{31} + a_{23}a_{31})}$$

Putting this value into the last equilibrium equation finally gives

$$x_4^* = \left(\frac{Aa_{34}(ka_{21} + ka_{23} + a_{12}a_{23} + a_{21}a_{13} + a_{23}a_{13})}{ka_{43}(a_{21}a_{32} + a_{21}a_{31} + a_{23}a_{31})}\right)^3.$$

Appendix B. Local stability analysis

The Jacobian of system of equations (1),(2),(3),(4) is

$$J = \begin{pmatrix} J_{11} & a_{21} & a_{31} & 0 \\ a_{12} & -(a_{21} + a_{23}) & a_{32} & 0 \\ & a_{13} \quad a_{23} & J_{33} & J_{34} \\ & 0 \quad 0 & a_{34}x_4^{\frac{2}{3}} & J_{44} \end{pmatrix}$$

with

$$J_{11} = -(a_{12} + k + a_{13})$$

$$J_{33} = -(a_{32} + a_{31}) - a_{34}x_4^{\frac{2}{3}}$$

$$J_{34} = \frac{-2}{3}a_{34}x_3x_4^{\frac{1}{3}} + a_{43}$$

$$J_{44} = \frac{2}{3}a_{34}x_3x_4^{\frac{-1}{3}} - a_{43}$$

There is a singularity in it when $x_4 = 0$, so this case, corresponding to the point E, must be analyzed starting from the original system. The fourth equation of the system can be rewritten as

$$\frac{dx_4}{dt} = a_{34}x_3x_4^{\frac{2}{3}} - a_{43}x_4 = a_{34}(x_3 - \widehat{x}_3)x_4^{\frac{2}{3}} + x_4^{\frac{2}{3}}\left[a_{34}\widehat{x}_3 - a_{43}x_4^{\frac{1}{3}}\right]$$

so that for x_3 near the equilibrium, the first term is negligible, and for

$$x_4 < \left(\frac{a_{34}\widehat{x_3}}{a_{43}}\right)^3$$

The dominant term is the last one, and it is positive, indicating that E is unstable. For coexistence, $J(E^*)$ is almost a full matrix. We could write down the Routh-Hurwitz conditions for stability, but they would be too much involved to shed any light on the problem. Rather, simulations demonstrate that this point can be stably attained.

Appendix C. Simulations of parameters variation

Figures of the simulations changing parameters a_{13}, a_{31}, and a_{21}. See Fig. 1a–3a

References

[1] 2022 Alzheimer's disease facts and figures. Alzheimer's & Dementia 2022;18: 700–89. https://doi.org/10.1002/alz.12638.

[2] Jack CR, Knopman DS, Jagust WJ, Petersen RC, Weiner MW, Aisen PS, et al. Tracking pathophysiological processes in Alzheimer's disease: an updated hypothetical model of dynamic biomarkers. Lancet Neurol 2013;12(2):207–16.

[3] Chen G-F, Xu T-H, Yan Y, Zhou Y-R, Jiang Yi, Melcher K, et al. Amyloid beta: structure, biology and structure-based therapeutic development. Acta Pharmacol Sin 2017;38(9):1205–35.

[4] Prelli F, Castano E, Glenner GG, Frangione B. Differences between vascular and plaque core amyloid in Alzheimer's disease. J Neurochem 1988;51:648–51. https://doi.org/10.1111/j.1471-4159.1988.tb01087.x.

[5] Phillips JC. Why Aβ42 Is much more toxic than Aβ40. ACS Chem Neurosci 2019;10: 2843–7. https://doi.org/10.1021/acschemneuro.9b00068.

[6] Delaby C, Estellés T, Zhu N, Arranz J, Barroeta I, Carmona-Iragui M, et al. The Aβ1–42/Aβ1–40 ratio in CSF is more strongly associated to tau markers and clinical progression than Aβ1–42 alone. Alzheimer's Res Ther 2022;14(1). https://doi.org/10.1186/s13195-022-00967-z.

[7] Kayed R, Head E, Thompson JL, McIntire TM, Milton SC, Cotman CW, et al. Common structure of soluble amyloid oligomers implies common mechanism of pathogenesis. Science 2003;300(5618):486–9.

[8] Selkoe DJ, Hardy J. The amyloid hypothesis of Alzheimer's disease at 25 years. EMBO Mol Med 2016;8:595–608. https://doi.org/10.15252/emmm.201606210.

[9] Andrade-Guerrero J, Santiago-Balmaseda A, Jeronimo-Aguilar P, Vargas-Rodríguez I, Cadena-Suárez AR, Sánchez-Garibay C, et al. Alzheimer's disease: an updated overview of its genetics. Int J Mol Sci 2023;24:3754. https://doi.org/10.3390/ijms24043754.

[10] Zlokovic BV, Yamada S, Holtzman D, Ghiso J, Frangione B. Clearance of amyloid β-peptide from brain: transport or metabolism? Nat Med 2000;6:718. https://doi.org/10.1038/77397.

[11] Spies PE, Verbeek MM, van Groen T, Claassen JAHR. Reviewing reasons for the decreased CSF Abeta42 concentration in Alzheimer disease. Front Biosci-Landmark 2012;17:2024. https://doi.org/10.2741/4035.

[12] Elbert DL, Patterson BW, Lucey BP, Benzinger TLS, Bateman RJ. Importance of CSF-based Aβ clearance with age in humans increases with declining efficacy of blood-brain barrier/proteolytic pathways. Commun Biol 2022;5:1–13. https://doi.org/10.1038/s42003-022-03037-0.

[13] Deane R, Bell RD, Sagare A, Zlokovic BV. Clearance of Amyloid-β Peptide Across the Blood-Brain Barrier: Implication for Therapies in Alzheimers Disease. CNS & Neurological Disorders - Drug Targets n.d.;8:16–30.

[14] Wang D, Chen F, Han Z, Yin Z, Ge X, Lei P. Relationship between Amyloid-β deposition and blood-brain barrier dysfunction in Alzheimer's disease. Front Cell Neurosci 2021;15.

[15] Deane R, Wu Z, Zlokovic BV. RAGE (Yin) versus LRP (Yang) balance regulates Alzheimer Amyloid β-Peptide clearance through transport across the blood-brain barrier. Stroke 2004;35:2628–31. https://doi.org/10.1161/01.STR.0000143452.85382.d1.

[16] Govindpani K, McNamara LG, Smith NR, Vinnakota C, Waldvogel HJ, Faull RLM, et al. Vascular dysfunction in Alzheimer's disease: a prelude to the pathological process or a consequence of it? J Clin Med 2019;8(5):651. https://doi.org/10.3390/jcm8050651.

[17] Jagust WJ, Landau SM. Initiative for the ADN. Temporal dynamics of β-amyloid accumulation in aging and Alzheimer disease. Neurology 2021;96:e1347–57. https://doi.org/10.1212/WNL.0000000000011524.

[18] Wang Z, Sharda N, Curran GL, Li L, Lowe VJ, Kandimalla KK. Semimechanistic population pharmacokinetic modeling to investigate amyloid beta trafficking and accumulation at the BBB endothelium. Mol Pharm 2021;18(11):4148–61.

[19] Dayeh MA, Livadiotis G, Elaydi S. A discrete mathematical model for the aggregation of β-Amyloid. PLoS One 2018;13:e0196402. https://doi.org/10.1371/journal.pone.0196402.

[20] Hoore M, Khailaie S, Montaseri G, Mitra T, Meyer-Hermann M. Mathematical model shows how sleep may affect amyloid-β fibrillization. Biophys J. 2020;119: 862–72. https://doi.org/10.1016/j.bpj.2020.07.011.

[21] Ficiarà E, D'Agata F, Cattaldo S, Priano L, Mauro A, Guiot C. A compartmental model for the iron trafficking across the blood-brain barriers in neurodegenerative diseases. In: 2021 43rd Annual International Conference of the IEEE Engineering in Medicine Biology Society (EMBC); 2021. p. 4200–3. https://doi.org/10.1109/EMBC46164.2021.9629893.

[22] Ficiarà E, D'Agata F, Ansari S, Boschi S, Rainero I, Priano L, et al. A mathematical model for the evaluation of iron transport across the blood-cerebrospinal fluid barrier in neurodegenerative diseases. In: 2020 42nd Annual International Conference of the IEEE Engineering in Medicine Biology Society (EMBC); 2020. p. 2270–3. https://doi.org/10.1109/EMBC44109.2020.9175988.

[23] Teunissen CE, Chiu M-J, Yang C-C, Yang S-Y, Scheltens P, Zetterberg H, et al. Plasma Amyloid-β (Aβ 42) correlates with cerebrospinal Fluid Aβ 42 in Alzheimer's disease. J Alzheimer's Dis 2018;62(4):1857–63.

[24] Storck SE, Meister S, Nahrath J, Meißner JN, Schubert N, Spiezio AD, et al. Endothelial LRP1 transports amyloid-β_{1-42} across the blood-brain barrier. J Clin Invest 2016;126:123–36. https://doi.org/10.1172/JCI81108.

[25] Ovod V, Ramsey KN, Mawuenyega KG, Bollinger JG, Hicks T, Schneider T, et al. Amyloid β concentrations and stable isotope labeling kinetics of human plasma specific to central nervous system amyloidosis. Alzheimer's Dementia 2017;13(8): 841–9.

[26] Ficiarà E, Boschi S, Ansari S, D'Agata F, Abollino O, Caroppo P, et al. Machine learning profiling of Alzheimer's disease patients based on current cerebrospinal fluid markers and iron content in biofluids. Front Aging Neurosci 2021;13. https://doi.org/10.3389/fnagi.2021.607858.

[27] Lue L-F, Sabbagh MN, Chiu M-J, Jing N, Snyder NL, Schmitz C, et al. Plasma levels of Aβ42 and tau identified probable Alzheimer's dementia: findings in two cohorts. Front Aging Neurosci 2017;9.

[28] Zaretsky DV, Zaretskaia MV, Molkov YI. Initiative for the ADN. patients with Alzheimer's disease have an increased removal rate of soluble beta-amyloid-42. PLoS One 2022;17:e0276933. https://doi.org/10.1371/journal.pone.0276933.

[29] Fagan AM. What does it mean to be 'amyloid-positive'? Brain 2015;138:514–6. https://doi.org/10.1093/brain/awu387.

[30] Villemagne VL, Burnham S, Bourgeat P, Brown B, Ellis KA, Salvado O, et al. Amyloid β deposition, neurodegeneration, and cognitive decline in sporadic Alzheimer's disease: a prospective cohort study. Lancet Neurol 2013;12(4):357–67.

[31] Roberts BR, Lind M, Wagen AZ, Rembach A, Frugier T, Li Q-X, et al. Biochemically-defined pools of amyloid-β in sporadic Alzheimer's disease: correlation with amyloid PET. Brain 2017;140:1486–98. https://doi.org/10.1093/brain/awx057.

[32] Hampel H, Hardy J, Blennow K, Chen C, Perry G, Kim SH, et al. The Amyloid-β Pathway in Alzheimer's disease. Mol Psychiatry 2021;26(10):5481–503.

[33] Patterson BW, Elbert DL, Mawuenyega KG, Kasten T, Ovod V, Ma S, et al. Age and amyloid effects on human central nervous system amyloid-beta kinetics. Ann Neurol 2015;78(3):439–53.

[34] Pahnke J, Langer O, Krohn M. Alzheimer's and ABC transporters — new opportunities for diagnostics and treatment. Neurobiol Dis 2014;72:54–60.

[35] Cheng Y, Tian D-Y, Wang Y-J. Peripheral clearance of brain-derived Aβ in Alzheimer's disease: pathophysiology and therapeutic perspectives. Transl Neurodegeneration 2020;9(16). https://doi.org/10.1186/s40035-020-00195-1.